A STRATOSPHERIC SOURCE OF REACTIVE NITROGEN IN THE UNPOLLUTED TROPOSPHERE

H. Levy II, J. D. Mahlman, and W. J. Moxim

A STRATOSPHERIC SOURCE OF REACTIVE NITROGEN IN THE UNPOLLUTED TROPOSPHERE

H. Levy II, J. D. Mahlman, and W. J. Moxim

Geophysical Fluid Dynamics Lab/NOAA, Princeton, New Jersey 08540

Abstract. A GFDL 3-D global generalized tracer field is adapted to provide a preliminary simulation of the reactive nitrogen (NOY) climatology in an unpolluted troposphere which has, as its sole source, downward transport of stratospheric NOY. The tracer field is scaled so that its downward cross-tropopause flux is balanced by the stratospheric production of NOY. While the model results show stratospheric NOY to be a significant source for the remote troposphere, they do not rule out additional contributions from either the long-range transport of combustion NOY or the insitu production by lightning. The model NOY climatology in the unpolluted troposphere shows a strong interhemispheric asymmetry due to greater downward NOY flux in the northern hemisphere and a steep drop off to a minimum in the tropics resulting from a combination of model features (tropical rainbelt, ITCZ, and Indian monsoon) which have been well documented in the real atmosphere.

Introduction

Recent simultaneous measurements of NO and HNO_3 mixing ratios in the equatorial Pacific surface atmosphere have ranged from 0.002 ppbv to 0.006 ppbv for NO (McFarland et al., 1979) and from 0.014 ppbv to 0.039 ppbv for HNO_3 (Huebert, 1980). These values are much lower than previous measurements in the presumedly unpolluted troposphere and suggest that the natural background level of reactive nitrogen compounds (NOY) is very low.

The current global estimates of tropospheric NOY production are dominated by a combustion source of approximately 20 tg N yr^{-1} (based on Robinson and Robbins, 1970) and a lightning source for which calculated values range from 40 tg N yr^{-1} (Chameides, et al., 1977) to 3-4 tg N yr^{-1} (Tuck, 1976; Dawson, 1980; Hill, Rinker, and Wilson, 1980). However, given the highly non-uniform distribution of these two major global sources, the probable containment of the combustion NOY within its source region (Huebert and Lazrus, 1978; 1980), and the uncertainties in the lightning source calculation (Dawson, 1980; Hill, Rinker, and Wilson, 1980), we wish to determine if downward transport of NOY from the stratosphere (.5-1.0 tg N yr^{-1}) is sufficient to maintain the very low values recently observed in the remote troposphere. A preliminary estimate of the importance of such a source to the NOY budget in the unpolluted troposphere is obtained by scaling the results of an earlier GFDL 3-D global tracer experiment which had a stratospheric source and tropospheric sink (Mahlman, 1973; Mahlman, Levy, and Moxim, 1980, hereafter called MLM). The resulting tropospheric tracer distribution provides an

estimate of the July time-mean NOY mixing ratios in the equatorial Pacific for comparison with recent observations. The climatology of model NOY resulting from a stratospheric source is also discussed and the controlling meteorological processes are identified.

Model Description and Experimental Design

The model used for this study solves numerically the continuity equation for a generalized tracer with a source in the top level and a sink in the troposphere (Mahlman, 1973; MLM). The required input data is generated by a GFDL general circulation model (Manabe, Hahn, and Holloway, 1974). The grid structure utilizes 11 terrain-following (sigma) surfaces in the vertical with standard heights of 31.4, 22.3, 18.8, 15.5, 12.0, 8.7, 5.5, 3.1, 1.5, 0.52, and 0.08 km. The horizontal grid dimension is approximately 265 km. A detailed description of the model is given in Mahlman and Moxim (1978).

We recognize that over 80% of the stratospheric production of NOY occurs in the top model level, that the tropospheric tracer distribution is almost completely insensitive to the spatial structure of the middle-stratosphere source (MLM), and that the model's wet and dry removal in the troposphere are appropriate sinks for NOY. Therefore, we believe that the tropospheric distributions generated by the "Stratified Tracer" experiment of MLM will adequately simulate the climatology of that fraction of tropospheric NOY which originates in the stratosphere. The experimental design of this preliminary NOY simulation is discussed in terms of the "Stratified Tracer" experiment. However, to avoid difficulties arising from a change in computers, the tropospheric tracer distributions from the companion tracer study in MLM, differing only in the distribution of tracer and sources in the top level, are used in the later section on model results. There is no significant difference between the two tropospheric tracer distributions and their dominant transport features (MLM).

The model sink consists of dry removal in the boundary layer and wet removal, proportional to both local precipitation rate and tracer amount, up to 8.7 km. Details of the formulation are given in an earlier paper on the simulation of radioactive fallout (Mahlman and Moxim, 1978), while the latitude dependence of tracer deposition is discussed by Mahlman (1973). The global NOY lifetime (NOY mass/NOY removal rate) in the surface layer is 18 days. The zonal mean values, ranging between 15-20 days at most latitudes, have a maximum of 40-80 days in the arid polar regions and a minimum of 10 days in the tropical rainbelt. While these tropical lifetimes are significantly longer than the recent estimate of a few days by Huebert (1980), it must be remembered that the

model values are based on a global data set
that has been both time and space averaged.
The local rainout lifetime is highly variable
and, for a rainfall rate of 0.1 cm/hr, drops to
2 days. While both dry and wet removal pro-
cesses apply mainly to the HNO_3 fraction of
NOY, photochemical steady-state calculations
(Levy, 1972) predict that HNO_3 predominates in
the lower troposphere where most removal takes
place. Dry removal, which dominates the glo-
bal rate in the surface level though not the
local rate during rain, may have been under-
estimated for the HNO_3 fraction which is highly
soluble and reactive.[3] While there is consider-
able uncertainty in any quantitative estimate
of dry and wet removal efficiency, they are the
correct physical processes.

The mixing ratio in the top level is speci-
fied to be constant everywhere. This amounts
to a source which instantaneously responds to
any net transport out of the top level. Be-
cause the model's sink mechanism is a linear
function of the local tracer mixing ratio, the
ratios of the constant value in the top level
to those at lower levels are independent of
the actual value chosen for the top level.
Therefore the vertical and horizontal struc-
ture in the tracer field is also independent of
the constant value chosen for the top level.

The generalized tracer field is converted to
an NOY field by a scaling factor which brings
the NOY downward flux, a product of the strato-
spheric NOY mixing ratio and the model's gener-
alized downward flux, into steady state balance
with the stratospheric NOY production rate, a
purely photochemical quantity.

Using the solar flux data of Simon (1978);
the O_3 and O_2 absorption coefficients tabulated
by Ackerman (1971); the recent NASA (1979) ta-
bulation of $O(^1D)$ reaction data; and a pre-
viously calculated 3-D N_2O distribution (Levy,
Mahlman, and Moxim, 1979), we calculate a global
time-mean NOY production rate of 1.4×10^8 mole-
cules $cm^{-2} sec^{-1}$. Use of the temperature depend-
ent absorption data of Selwyn, Podolske, and
Johnston (1977) would have increased the strato-
spheric N_2O mixing ratio and NOY production. In
a recent calculation, Johnston, Serang, and
Podolske (1979) found a production rate of
2.7×10^8 molecules $cm^{-2} sec^{-1}$. Most of the dis-
agreement can be explained by differences in
solar fluxes, N_2O and O_3 fields, and the absol-
ute quantum yield for $O(^1D)$. It is not clear
which, if either, calculation is correct. We
believe that the two results typify the existing
uncertainty in an NOY source calculation and
will use ours to determine the scaling factor.
Neither calculation included possible upper at-
mosphere sources and sinks of NO.

From the 3-D numerical experiments of MLM
we calculate a generalized global downward
flux into the troposphere of 5.6×10^{10} mole-
cules $cm^{-2} sec^{-1}$ for a tracer with a mid-
stratosphere source and an arbitrary 2.8 ppmv
mixing ratio at 22.3 km. To balance the
downward flux and the NOY stratospheric pro-
duction rate we scale the tracer field by
2.5×10^{-3}. This results in global mean stra-
tospheric NOY mixing ratios, R(NOY), of 19
ppbv at 31.4 km and 7 ppbv at 22.3 km, and a
downward flux of $(2.5 \times 10^{-3}) \times (5.6 \times 10^{10})$

molecules $cm^{-2} sec^{-1} = 1.4 \times 10^8$ molecules cm^{-2}
sec^{-1} which balances the stratospheric pro-
duction rate. It should be noted that the
model's surface NOY mixing ratios depend lin-
early on the calculated production rate and
somewhat less than linearly on the tropo-
spheric removal efficiency.

Model Results

A pronounced feature of the model tropo-
spheric distribution of R(NOY) is its strong
interhemispheric asymmetry. The model's ratio
of northern to southern hemisphere mixing
ratios is 1.65. This is due, in large part,
to the greater downward transport into the
troposphere in the northern hemisphere. The
ratio of the northern to southern hemisphere
downward tracer fluxes is 1.80 (MLM). Al-
though the degree of cross-tropopause mass
exchange is comparable in the hemispheres,
the much weaker downward transport from the
model's middle stratosphere in the southern
hemisphere provides much lower NOY mixing
ratios in the lower stratosphere for ex-
change with the model's troposphere in the
southern hemisphere (Manabe and Mahlman,
1976; MLM). A latitude-altitude plot of
the zonal-mean "Stratified Tracer" mixing
ratio (see Fig. 3.2b-July in MLM and multi-
ply all numbers by 2.5×10^{-3}) clearly shows
the asymmetry with a maximum in the north-
ern high latitudes and a minimum bulging up
to 5·km from the tropics to the southern
midlatitudes.

For comparison with recent measurements,
the July time-mean NOY mixing ratios,
$\overline{R(NOY)}^t$, generated in the model's surface
level are given in Figure 1. The dominant fea-
ture is the steep gradient that forms north of
the equator. A major cause of the tropical
minimum is the model's tropical rainbelt which
efficiently removes most water soluble tracers
transported to the tropics. The model's trop-
ical rainbelt is in good agreement with obser-
vation (Manabe and Holloway, 1975).

Some aspects of the transport processes which
are involved in the horizontal tracer structure
at the surface are shown in Figure 2, the July
time-mean streamlines of the surface (80 m) wind
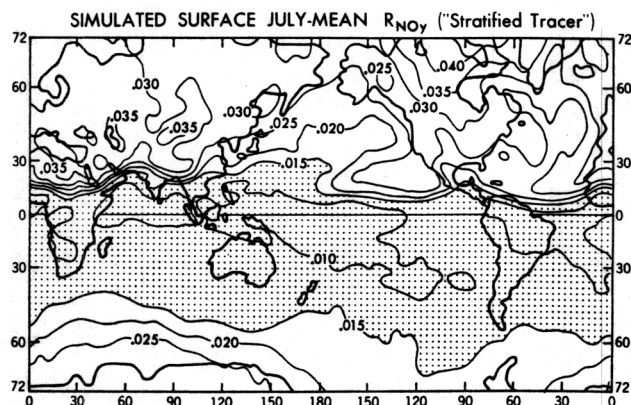fields used by the tracer model. Rainout in

SIMULATED SURFACE JULY-MEAN R_{NO_Y} ("Stratified Tracer")

Fig. 1. Model July $\overline{R(NOY)}^t$ (ppbv) at 80 m
above the surface.

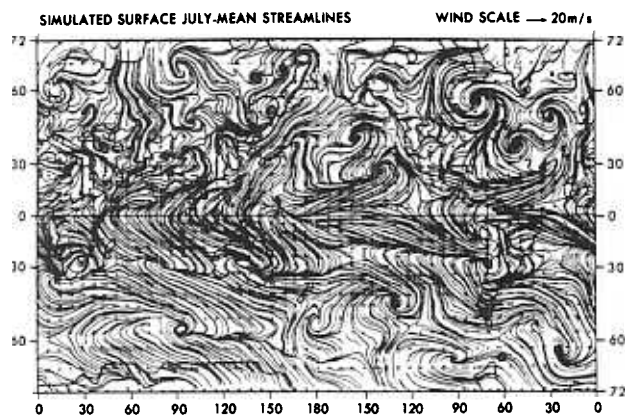SIMULATED SURFACE JULY-MEAN STREAMLINES   WIND SCALE —→ 20m/s

Fig. 2. July time-mean stream lines of the wind fields used by the tracer model in its surface level. The arrows show local wind vectors with length proportional to speed as indicated at upper right.

conjunction with the strong convergence of easterlies across the tropical Atlantic and eastern Pacific (ITCZ) produces the steep tracer gradient and minimum in those regions. Figure 2 further shows a strong southerly monsoon flow across the equator in the Indian Ocean. This flow brings air with low R(NOY) northward and moves the steep gradient out of the tropics to the southern edge of the Himalayan plateau. There is no particularly strong flow across Africa and South America shown in Figure 2, but the tropical rain belt effectively removes any NOY entering the tropics and thereby maintains the gradient and minimum. In the model western Pacific there is a strong southerly flow across the equator and an active generation of cyclonic disturbances in the subtropics (Manabe, Hahn, and Holloway, 1974). The net effect of these disturbances is to mix NOY-poor air northward into the mid-latitudes and produce a much more diffuse gradient across the western Pacific.

It should be noted that the tropical minimum is quite broad and spreads to the southern mid-latitudes. The much weaker simulated maximum in the southern high latitudes is a result of the much weaker downward flux as discussed earlier.

A local model feature of Figure 1 is the maximum over central Canada. This is caused by the downward transport of NOY-rich air on the west side of a strong tropospheric low formed over eastern Canada (see Figure 2).

In the model winter, while the interhemispheric asymmetry of the January surface $\overline{R(NOY)}^t$ field (see Figure 3) is relatively unchanged, the steep gradient has moved southward to the equator. The January time-mean streamlines of the model's surface wind field (see Figure 4) show that the ITCZ across the Atlantic and eastern Pacific has also shifted southward to the equator and that the Indian monsoon flow has reversed from southerly to northerly. These changes in the tropical wind fields combined with the related southerly shift of the tropical rainbelt cause the southerly shift of the $\overline{R(NOY)}^t$ gradient. With a decrease in the generation of cyclonic disturbances in the western Pacific (Manabe, Hahn, and Holloway, 1974),

the model's gradient in that region is more sharply defined. The model dynamics and hydrology in the tropics and a comparison with meteorological data have already been presented by Manabe, Hahn, and Holloway, (1974).

Comments and Conclusions

While the lowest NOY values measured over the equatorial Pacific are in reasonable agreement with model predictions, many of the HNO_3 measurements (Huebert, 1980) exceed model tropical values for total NOY by a factor of two. Although the model results are time-mean values, local variability is not sufficient to explain the difference. The calculated absolute values are sensitive to errors in the calculation of stratospheric production, cross-tropopause flux, and tropospheric removal efficiency. This uncertainty in the calculation, when combined with the difficulty in making accurate absolute measurements of such small mixing ratios, suggests that a comparison between relative features may be more significant. While the interhemispheric asymmetry and sharp drop off to a minimum in the tropics have not yet been observed in the atmosphere (Huebert and Lazrus, 1979), that may be due to the detection limits being too high. The model predicts NOY increasing with altitude in agreement with Huebert and Lazrus (1979).

At this time the downward transport of stratospheric NOY, while apparently an important source in the remote troposphere, has not been shown to be the sole source. If, with more measurements, the predicted steep drop off and minimum in the tropics are not observed, one may conclude that there is either an insitu natural source such as lightning or contamination by transport of HNO_3 (Chameides, 1978) or organic nitrates (Crutzen, 1979) from combustion source regions. While Orville and Spencer (1979) found that the incidence of lightning had a strong maximum at the equator, they also found that it was much more frequent over land than ocean. Questions concerning the magnitude of NOY production in lightning and its lifetime once produced have not yet been resolved. Measurements of nitrate content in rainwater and their latitude dependence, with emphasis on the unpolluted troposphere, would help in determining both the strength and distribution of the lightning
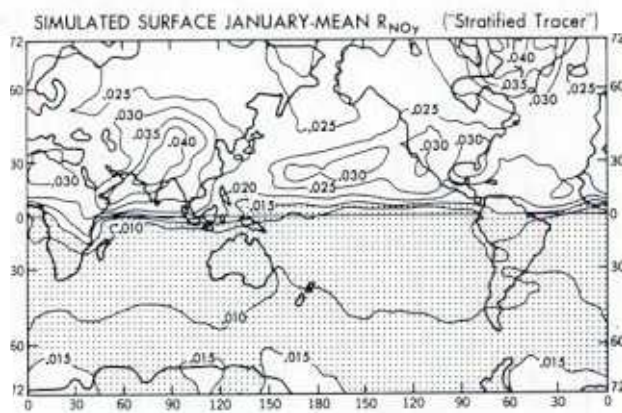
SIMULATED SURFACE JANUARY-MEAN R_{NOy} ("Stratified Tracer")

Fig. 3. January $\overline{R(NOY)}^t$ (ppbv) at 80 m above the surface.

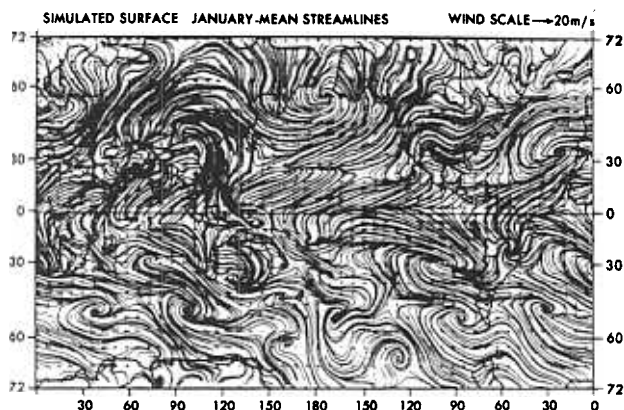SIMULATED SURFACE JANUARY-MEAN STREAMLINES   WIND SCALE →20m/s

Fig. 4. The same as Figure 2 except for January.

source and the extent of contamination of the remote troposphere by combustion sources. Since both the stratospheric and combustion sources produce more NOY in the northern troposphere, the lack of an interhemispheric gradient in future measurements would be significant.

We are beginning a series of numerical experiments to unravel the contribution of stratospheric NOY, anthropogenic combustion, and lightning to the NOY tropospheric climatology and budget and will be looking forward to more measurements of NOX, HNO_3, and nitrate rainout in the "unpolluted" troposphere.

References

Ackerman, M., Ultraviolet solar radiation related to mesospheric processes, Mesospheric Models and Related Experiments, D. Reidel, 149-159, 1971.

Chameides, W. L., The photochemical role of tropospheric nitrogen oxides, Geophys. Res. Lett., 5, 17-20, 1978.

Chameides, W. L., D. H. Stedman, R. R. Dickerson, D. W. Rusch, and R. J. Cicerone, NO_x production in lightning, J. Atmos. Sci., 34, 143-149, 1977.

Crutzen, P. J., The role of NO and NO_2 in the chemistry of the troposphere and stratosphere, Ann. Rev. Earth Planet. Sci., 7, 443-472, 1979.

Dawson, G. A., Nitrogen fixation by lightning, J. Atmos. Sci., 37, 174-178, 1980

Huebert, B. J., Nitric acid and aerosol nitrate measurements in the equatorial Pacific region, submitted to Geophys. Res. Lett., 1980.

Huebert, B. J., and A. L. Lazruz, Global tropospheric measurements of nitric acid vapor and particulate nitrate, Geophys. Res. Lett., 5, 577-580, 1978.

Huebert, B. J. and A. L. Lazrus, Tropospheric gas-phase and particulate nitrate measurements, J. Geophy. Res., to be published 1980.

Hill, R. D., R. G. Rinker, and H. D. Wilson, Atmospheric nitrogen fixation by lightning, J.

Atmos. Sci., 37, 179-192, 1980.

Johnston, H. S., O. Serang, and J. Podolske, Instantaneous global nitrous oxide photochemical rates, J. Geophys. Res., 84, 5077-5082, 1979.

Levy II, H., Photochemistry of the lower troposphere, Planet. Space Sci., 20, 919-935, 1972.

Levy II, H., J. D. Mahlman, and W. J. Moxim, A preliminary report on the numerical simulation of the three-dimensional structure and variability of atmospheric N_2O, Geophys. Res. Lett., 6, 155-158, 1979.

Mahlman, J. D., Prelim. results from a three-dimensional general-circulation/tracer model, Proc. Sec. Conf. CIAP, A. J. Broderick, Ed., 321-337, (DOT-TSC-OST-73-4), 1973.

Mahlman, J. D., H. Levy II, and W. J. Moxim, Three-dimensional tracer structure and behavior as simulated in two ozone precursor experiments, J. Atmos. Sci., , 655-685, 1980.

Mahlman, J. D., and W. J. Moxim, Tracer simulation using a global general circulation model: Results from a midlatitude instantaneour source experiment, J. Atmos. Sci., 35, 1340-1374, 1978.

Manabe, S., D. G. Hahn, and J. L. Holloway, Jr., The seasonal variation of the tropical circulation as simulated by a global model of the atmosphere, J. Atmos. Sci., 31, 43-83, 1974.

Manabe, S., and J. L. Holloway, Jr., The seasonal variation of the hydrologic cycle as simulated by a global model of the atmosphere, J. Geophys. Res., 80 1617-1649, 1975.

Manabe, S., and J. D. Mahlman, Simulation of seasonal and interhemispheric variations in the stratospheric circulation, J. Atmos. Sci., 33, 2185-2217, 1976.

McFarland, M., D. Kley, J. W. Drummond, A. L. Schmeltekopf, and R. H. Winkler, Nitric oxide measurements in the equatorial Pacific region, Geophy. Res. Lett., 6, 605-608, 1979.

NASA Reference Publication 1049, The stratosphere: present and future, Eds. Hudson, R. D. and E. I. Reed, Scientific and Technical Information Branch, NASA, 1979.

Orville, R. E. and D. W. Spencer, Global lightning flash frequency, Mon. Wea. Rev., 107, 934-943, 1979.

Robinson, E. and R. C. Robbins, Gaseous nitrogen compound pollutants from urban and natural sources, J. Air Pollution Control Assoc., 5, 303-306, 1970.

Selwyn, G., J. Podolske, and H. S. Johnston, Nitrous oxide ultraviolet absorption spectrum at stratospheric temperatures, Geophys. Res. Lett., 4, 427-430, 1977.

Simon, P. C., Irradiation solar flux measurements between 120 and 400 NM: current position and future needs, Planet. Space Sci. 26, 355-365, 1978.

Tuck, A. F., Production of nitrogen oxides by lightning discharges, Q. J. R. Meteorol. Soc. 102, 749-755, 1976.